https://doi.org/10.5194/nhess-2024-8
Preprint. Discussion started: 2 February 2024

Natural Hazards and Earth System Sciences
Open Access
Discussions

Characteristics of spatial and temporal distribution of heavy rainfall and surface runoff generating process in the mountainous areas of northern China

Hui Yang[a,*], Xianglong Hou[b] and Jiansheng Cao [a,*]

a. Key Laboratory of Agricultural Water Resources, Hebei Key Laboratory of Agricultural Water-Saving, Center for Agricultural Resources Research, Institute of Genetics and Developmental Biology, Chinese Academy of Sciences, Shijiazhuang 050001, China

b. Institute of Geographical Sciences, Hebei Academy of Sciences, Shijiazhuang 050011, China; Hebei Technology Innovation Center for Geographic Information Application, Shijiazhuang 050011, China

Abstract: The intensity and duration of precipitation play an important role in surface runoff processes. A hilly area may have more complicated runoff processes. In this study, the characteristics of annual rainfall from 1987 to 2023 in the Taihang Mountain were obtained by the Pearson-III frequency curve, homogeneity and MK test. Four surface runoff generation processes during 2014 to 2023 were monitored. The contribution of rainfall to changes in runoff were quantified based on the double cumulative curve method. Results showed that for the last decade, a significant upward trend in the frequency of moderate and heavy rainfall events. The spatial variability of rainfall in the Taihang Mountain and the influence of elevation are both smaller when the rainfall during 24 h is lower than 50 mm. The two surface runoff processes in 2016 and 2023 were typical runoff

*Corresponding author.
Email address: yanghui@sjziam.ac.n, caojs@sjziam.ac.cn

https://doi.org/10.5194/nhess-2024-8
Preprint. Discussion started: 2 February 2024

resulted from excess rain, which belonged to the storm runoff. The two surface runoff processes in 2021 were runoff generation under saturated condition. For runoff generation under saturated condition, the contribution of rainfall was only 58.17%. While when the runoff coefficient was greater than 0.5, the surface runoff generating processes were entirely determined by rainfall. This study suggested that for semi-arid regions, where rainfall is unevenly distributed over the seasons, more soil water is needed to maintain local and downstream water demand during the non-rainy season.

Key words: Heavy rainfall, surface runoff, storm runoff, soil and rock mountainous area, Taihang Mountain

1.Introduction

Surface runoff is an important component that plays essential role in soil erosion, nutrient transport, carbon transport, and many other processes (Fei et al., 2019; Jing et al., 2022; Fu et al., 2024). Surface runoff can reach the stream quickly, and thus it significantly influences the response of the streamflow to precipitation (Maier et al., 2021). Land-use and rainfall characteristics are two crucial influencing factors that affect the surface runoff process (Martínez-Mena et al., 2020). Among them, the intensity and duration of precipitation play an important role in ecohydrological processes (Ran et al., 2012). Rainfalls with greater intensity or duration result in a greater peak runoff, leading to greater total runoff in watersheds (Wei et al., 2014). Moreover, rainfall patterns and regimes are important factors in water conservation (Mohamadi and Kavian, 2015; Chen et al., 2018). Different rainfall regimes cause

https://doi.org/10.5194/nhess-2024-8
Preprint. Discussion started: 2 February 2024

different surface runoff (Zhao et al., 2022). Global warming and climate change as a result of greenhouse gases emissions trigger the frequent and intensive floods, flash floods, extreme storms occurrences with inundation consequences in urban and agricultural areas (Yavuz, 2020). Because of its marked effects on hydrological processes, climate change has attracted considerable attention from scientists and governments worldwide (Liu and Wang, 2012; Yoon et al., 2015; Zheng, et al., 2018; Ju et al., 2023).

A hilly area may have more complicated runoff processes than a plain area (Fu et al., 2023). The Taihang Mountain region is a typical soil and rocky mountainous area in northern China (Du et al., 2018), and a critical transition zone between the Loess Plateau and the North China Plain (Qi et al., 2023). As an important ecological barrier and water conversion area for the North China Plain and the Beijing-Tianjin region, China (Yang, 2021), the Taihang Mountain provides 3.6 billion m^3 of water to the North China Plain annually (Wang et al., 2014). Due to the high degree of heterogeneity of topography, geomorphology, rocks, soils, climate and vegetation (Geng et al., 2018) and variable climatic conditions, complex geography and intensive human activities (Zhang et al., 2021), the evolutionary regimes, influencing factors and driving mechanisms of hydrological processes are complex and subject to great spatial and temporal variability and uncertainty (Sakakibara et al., 2017). Therefore, it is essential to understand the characteristics of surface runoff generating process under different heavy rainfall events in the mountainous areas, especially in soil and rocky mountainous area where an ecologically fragile area with more complex rainfall-

https://doi.org/10.5194/nhess-2024-8
Preprint. Discussion started: 2 February 2024

infiltration processes (Zhang et al., 2021).

For the Haihe River Basin, China, most of whose tributaries originate from originates the Taihang Mountain, the amount of water resources in the mountainous areas of the Haihe River Basin has been reduced by 40% (Yang et al., 2023). Moreover, Jia et al. (2019) also showed that runoff in the Taihang Mountain has declined significantly since 2000, with surface water resources declining by more than 40% in the eastern region and even more than 50% in the Taihang Mountain of Hebei province, China. Most of these tributaries have become seasonal rivers, especially in the plains, basically all rivers are dry (Xia and Zhang, 2017). Although the average multi-year rainfall has little inter-annual variability with a value of 548 mm (Geng et al., 2019), extreme rainfall events are frequent, triggering a series of flooding disasters, which threaten ecological and water security locally and in the downstream plains, and cause great losses to people. From 1990 to 2020, global annual economic losses from floods have amounted to tens of billions of US dollars and thousands of lives have been lost each year (Hirabayashi et al., 2013; Najafi et al., 2021). As the atmospheric temperature increases and rainfall patterns change, variability in surface runoff processes is intensifying (Huntington, 2006; Pour et al., 2020), in particular, the infiltration and runoff generation processes in small watersheds on mountain slopes.

The objectives of this paper are to elucidate the processes and characteristics of surface runoff process under different heavy rainfall events in the small watersheds of the Taihang Mountains, to try to clarify the fact that the surface runoff process mode has been changed under the background of extreme rainfall, and to discuss the strategy

https://doi.org/10.5194/nhess-2024-8
Preprint. Discussion started: 2 February 2024

of guaranteeing the security of water resources in the Beijing-Tianjin-Hebei region, China. The results of the study are intended to provide new insights into the hydrological processes in the soil and rocky mountainous area, and to provide a scientific basis for the enhancement of the water conservation function in the Taihang Mountain area and the construction of water security in the Xiongan New Area, China.

2. Materials and methods

2.1 Study area

This study was carried out in the Taihang Mountain Ecological Experimental Station (TMS) of Chinese Academy of Sciences, China. The TMS (114°15'50"E, 37°52'44"N) with an altitude of 350 m is located in the mountainous areas upstream of Xiongan New Area, China and belongs to middle of the eastern Taihang Mountain in Yuanshi County, Shijiazhuang City, Hebei Province, northern China (Fig.1). The study area has a semi-arid continental monsoon climate with an annual average temperature is 13.0 ℃, and the water surface evaporation is 1200 mm. The average annual precipitation for long-term period (1987-2022) is 536.6 mm and more than 70% of the precipitation is mainly concentrated from June to September. The typical vegetation type is mainly 20-year-old secondary forest and scrub, the secondary forest is mainly Robinia pseudoacacia, and the shrubs are mainly Vervain Family and wild jujube (Cao et al., 2021). The hill slopes are composed of stratum characterized by "overlying soil and underlying rock". The overlying soil layer is thin, with a thickness of 20-50 cm and mainly constitutes of gravel. The thickness of the underlying rock layer, which is mainly a weathered layer of gneiss full of fissures, is 0.5-10 m (Cao et al., 2013).

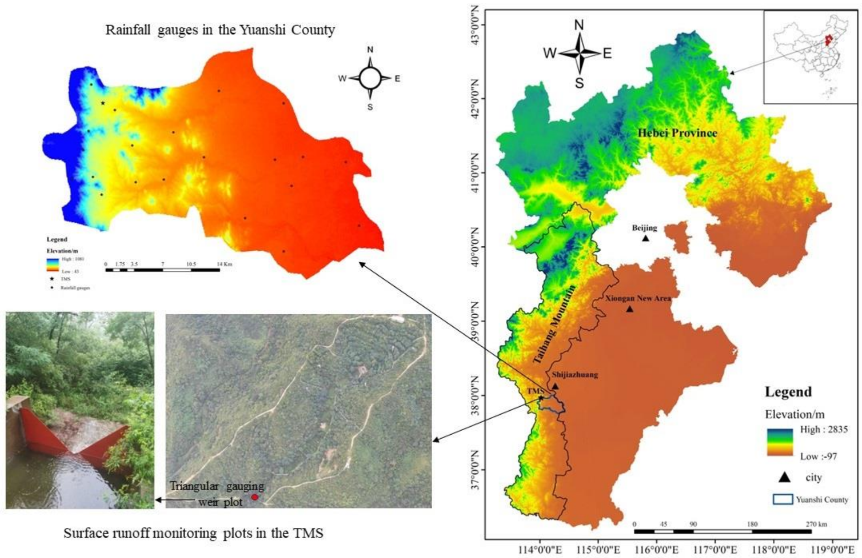

Fig. 1 Location of the study area

2.2 Rainfall monitoring

A tipping bucket self-recording digital rain gauge (Rain Collector II, Davis Instruments Corp., Hayward, CA, USA) was installed to measure the rainfall with a resolution of 0.25 mm (Fig.1). The time interval of data recording is 1 h. The different daily rainfall intensity was obtained using these monitoring data. According to the classification of different 24 h rainfall amounts by China Meteorological Administration, namely, 24-hour rainfall of less than 10 mm is considered light rain, 10 to 24.9 mm is considered moderate rain, 25 to 49.9 mm is considered heavy rain, and greater than or equal to 50 mm is considered rainstorm, and combined with the measured rainfall data meanwhile, we counted the proportion of total rainfall with rainfall intensity greater than 10 mm/24 h I_{10} and 25 mm/24 h I_{25} to the annual rainfall from 1987 to 2023.

https://doi.org/10.5194/nhess-2024-8
Preprint. Discussion started: 2 February 2024

Other rainfall data including 21 rainfall gauges in the Yuanshi County (Fig.1) were obtained from the Yuanshi county meteorological bureau.

2.3 Surface runoff monitoring

A self-recording water level gauge (HOBO U20-001-04, Onset Computer Corporation, Bourne, MA, USA) was arranged in a triangular gauging weir plot of the small watershed of the TMS (Fig.1) to determine the water level above the weir, which was measured every 1 h. In addition, the water level above the weir was manually performed during the same period of each runoff generation process to calibrate the measured data of the self-recording water gauge. The triangular gauging weir plot is a right-angled water measuring weir. According to Chen et al. (1984), the flow of surface runoff in the small watershed of the TMS was obtained using the water level over the weir by the following formula:

$$Q = 1.4\,H^{2.5} \qquad (1)$$

where Q and H are the flow at the small watershed outlet (L/s) and water level over the weir (m), respectively.

The following formula was used to calculate surface runoff of the small watershed of the TMS:

$$R = Q \times t / A \qquad (2)$$

where R, t and A are the surface runoff during 1 h at the watershed outlet (mm), 1 h and the area of the small watershed, 0.02625 km^2, respectively.

2.4 Homogeneity and trend test

Homogeneous time series are extremely important for trend analysis studies of hydro-meteorological variables, because the trends in them result from the changes in climate and air (Conrad and Pollak, 1950). Non-climatic changes may disrupt the homogeneity of the time series, and therefore, homogeneity test is required before trend analysis. We applied run homogeneity test for rainfall data is applied to determine the homogeneity of the data at 5% significance level before the trend analysis of annual rainfall with the following formula (Swed and Eisenhart, 1943):

$$Z_R = \frac{R_n - \frac{2N_1N_2}{N_1+N_2} + 1}{\sqrt{\frac{2N_1N_2(2N_1N_2-N)}{N^2(N-1)}}} \quad (3)$$

where Z_R is the run homogeneity test result, N is the number of data, R_n is the run number, N_1 (N_2) is number of lower (higher) values than the median.

If the calculated run homogeneity test result Z_R value corresponds to 5% significance level or below then the data is non-homogeneous. Herein, only homogeneous data are used to identify trend conditions (Yavuz, 2020).

The non-parametric Mann-Kendall (MK) trend test is widely used to assess the significance of monotonic trends in hydro-meteorological time series (Silva et al., 2015). In order to write increasing or decreasing expressions, the Mann-Kendall positive or negative Z_{MK} value is taken into consideration (Mann, 1945, Kendall, 1975). If $|Z_{MK}| \geq 2.576$, 1.96, 1.642 or 1.282, the null hypothesis of no trend is rejected at the 1%, 5%, 10% or 20% significance level respectively (Gocic and Trajkovic, 2013; Yavuz et al., 2020). Software MATLAB R2014a was used to MK trend test.

2.5 Runoff analysis

The runoff coefficient is a measure of the ability of a watershed to generate runoff (Zheng et al., 2021). The following formula was used to calculate the runoff coefficient:

https://doi.org/10.5194/nhess-2024-8
Preprint. Discussion started: 2 February 2024

$$RC = (R/P) \times 100\% \tag{4}$$

where RC and P are the runoff coefficient of the small watershed (%) and precipitation (mm), respectively.

Based on the measured data from the triangular gauging weir, only four surface runoff generating processes occurred in the small watershed of the TMS since 2014, namely, from July 19 to 24, 2016, July 20 to 25, 2021, October 3 to 10, 2021, and July 29 to August 4, 2023. Therefore, the analysis period of rainfall spatial characterization is the period of these four surface runoff generating processes. Combined with the location of the rainfall gauges, kriging interpolation with Arc GIS 10.5 was used to calculate the rainfall spatial distribution over the region of the TMS.

The double mass curve method is used to test the curves of two related cumulative variables, and is primarily used to detect the consistency and change in trends of long-term hydro-meteorological elements (Cheng et al., 2022). The linear regression equation of the baseline period double mass curve is established and further used to construct the change period equation. The relationship between observed cumulative runoff $\sum R_b$ and cumulative precipitation $\sum P_b$ (in the baseline period can be expressed as (Gao et al., 2017):

$$\sum R_b = a_1 \sum P_b + b_1 \tag{5}$$

The relationship between observed cumulative runoff $\sum R_c$ and cumulative precipitation $\sum P_c$ in the changing period can be expressed as:

$$\sum R_c = a_2 \sum P_c + b_2 \tag{6}$$

The runoff in the changing period $\sum R_a$ can be modelled as:

$$\sum R_a = a_1 \sum P_c + b_1 \quad (7)$$

where the parameters a_1 and a_2 are the rates of change in cumulative runoff with the change of accumulated precipitation, and b_1 and b_2 are the intercept values.

The contributions of precipitation on runoff ΔP (%) can be determined as below:

$$\Delta P = \frac{\overline{R_b} - \overline{R_a}}{\overline{R_b} - \overline{R_c}} * 100 \quad (8)$$

$$\overline{R_a} = \frac{\sum R_a}{T_c}, \overline{R_b} = \frac{\sum R_b}{T_b}, \overline{R_c} = \frac{\sum R_c}{T_c} \quad (9)$$

where $\overline{R_b}$ and $\overline{R_c}$ represent observed mean annual run-off for a certain time T_b and T_c in the baseline and changing period; $\overline{R_a}$ is modelled mean annual run-off for a certain time T_c in the changing period.

In this study, we set July 19 to 24, 2016 as the baseline period and the subsequent three runoff processes as the change period to determine the contribution of rainfall to runoff in the subsequent three runoff processes.

2.6 Other data analysis

The Pearson-III distribution (Singh, 1998) was utilized to analyze their frequency distribution. Depending on the P value, the annual rainfall patterns can be determined (Zhao et al., 2022), namely, wet years were defined as those with precipitation greater than or equal to P = 25 %, dry years were defined as those with precipitation less than or equal to P = 75 %, and normal years were defined as those when precipitation occurs between wet and dry years (Li et al., 2020).

Statistical analyses were carried out with IBM SPSS Statistics 20. Plotting of the Pearson-III frequency curve used to determine annual rainfall patterns (Zhao et al., 2022) and other processing and analysis of data and related graphing were done in

https://doi.org/10.5194/nhess-2024-8
Preprint. Discussion started: 2 February 2024

Microsoft Excel 2016.

3. Results

3.1 Annual rainfall characteristics

As shown in Fig. 2, the annual variation in precipitation in the TMS from 1987 to 2023 was large. Although the precipitation monitoring data for 2023 is only available till September, more than 70% of the precipitation is mainly concentrated from June to September. The average annual precipitation is 546.1 mm. The year with the least precipitation was 2014 (234.7 mm), while the year with the most was 1996 (1038.5 mm), followed by 2021 (1008.1 mm) and 2016 (929.2 mm), respectively.

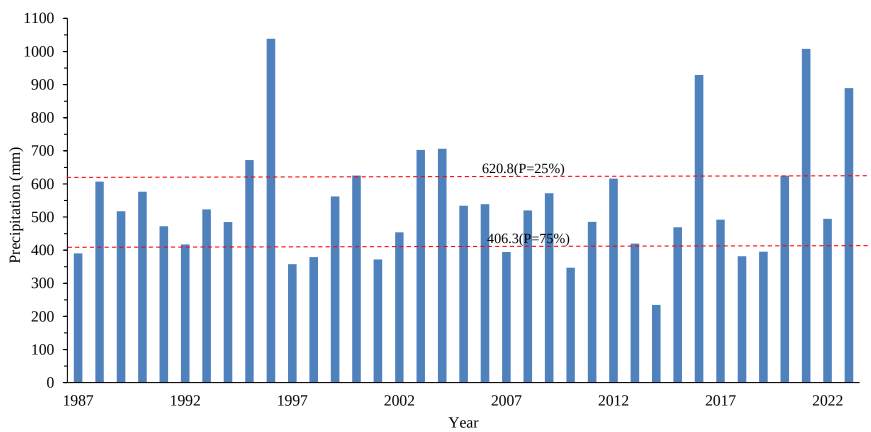

Fig. 2 Annual precipitation change in the TMS from 1987 to 2023

Using the Pearson-III frequency curve, a wet year is defined as one in which precipitation is greater than or equal to 620.8 mm and a dry year is defined as one in which precipitation is less than or equal to 406.3 mm. Therefore, the years 1995, 1996, 2000, 2003, 2004, 2016, 2020, 2021 and 2023 were wet years, the years 1987, 1997, 1998, 2001, 2007, 2010, 2014, 2018 and 2019 were dry years, and the remaining 19

https://doi.org/10.5194/nhess-2024-8
Preprint. Discussion started: 2 February 2024

years were normal years. It appears that 51.4% of the years have a normal rainfall year, and for the last decade (2014-2023), wet years and dry years account for 40% and 30%, respectively. Frequency of extreme weather years is dominant from 2014 to 2023.

Further, precipitation from June to September is plotted as a proportion of annual precipitation, as well as precipitation with daily precipitation intensity greater than I_{10} and I_{25} as a proportion of annual precipitation in the TMS from 1987 to 2023 (Fig.3). Precipitation from June to September accounted for 72.3% of the annual precipitation from 1987 to 2023. Meanwhile, precipitation with daily precipitation intensity greater than I_{10} and I_{25} accounted for 72.8% and 50.5% of the annual precipitation, respectively.

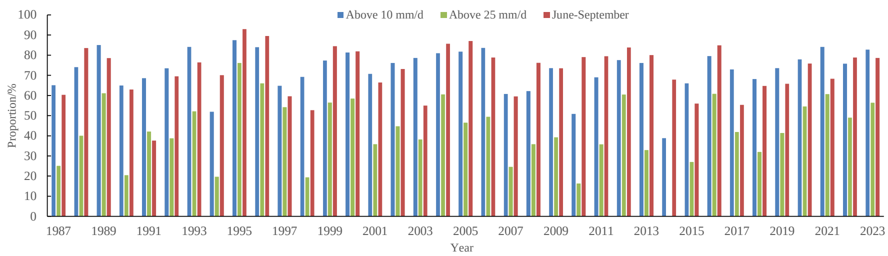

Fig. 3 Proportion of precipitation from June to September, daily precipitation intensity above I_{10} and I_{25} of annual precipitation in the TMS from 1987 to 2023

Based on equation 3, the results of the homogeneity test were obtained for 1987 to 2023, and the values Z_R for all the data ranged from 0.06 to 0.27, i.e., all the data passed the homogeneity test.

MK test was performed for total rainfall, total rainfall with daily rainfall intensity greater than I_{10} and I_{25} for the years 1987-2023, and total rainfall, total rainfall with daily rainfall intensity greater than I_{10} and I_{25} for the years 2014-2023, respectively, and the Z_{MK} results are shown in Table 1. Despite the upward trend in all data, total rainfall

https://doi.org/10.5194/nhess-2024-8
Preprint. Discussion started: 2 February 2024

with daily rainfall intensity greater than I_{10} and I_{25} for the years 2014-2023 passed the test of significance at the 5% and 10% levels, respectively. It suggests a significant upward trend in the frequency of moderate and heavy rainfall events between 2014 and 2023.

Table 1 The values Z_{MK} of total rainfall, total rainfall with daily rainfall intensity greater than I_{10} and I_{25} for the years 1987-2023, and total rainfall, total rainfall with daily rainfall intensity greater than I_{10} and I_{25} for the years 2014-2023

Test item	Total rainfall from 1987-2023	Above I_{10} from 1987-2023	Above I_{25} from 1987-2023	Total rainfall from 2014-2023	Above I_{10} from 2014-2023	Above I_{25} from 2014-2023
Z_{MK}	0.405	0.196	0.0392	1.61	2.33**	1.79*

** Statistically significant trends at the 5% significance level. * Statistically significant trends at the 10% significance level.

3.2 Rainfall spatial characteristics

From the above, it can be seen that during 2014-2023, only four surface runoff generating processes occurred in the small watershed of the TMS. Therefore, we further analyze the spatial distribution characteristics of rainfall for these four runoffs generating processes. As shown in Fig. 4, except for this runoff generating process from October 3 to 10, 2021, the rainfall spatial distribution of the remaining three runoff generating processes is more obvious. The variance coefficient of the total rainfall at each rainfall gauges during October 3 to 10, 2021 is only 5.96%, while for other three rainfalls, the variance coefficient values are all greater than 30%. Especially the two

https://doi.org/10.5194/nhess-2024-8
Preprint. Discussion started: 2 February 2024

Natural Hazards and Earth System Sciences
Discussions

rainfalls of July 19 to 24, 2016 and July 29 to August 4, 2023, the rainfall dividing line of rainfall greater than 200 mm in July 19 to 24, 2016 and 250 mm July 29 to August 4, 2023 basically coincides with the 100 m contour line.

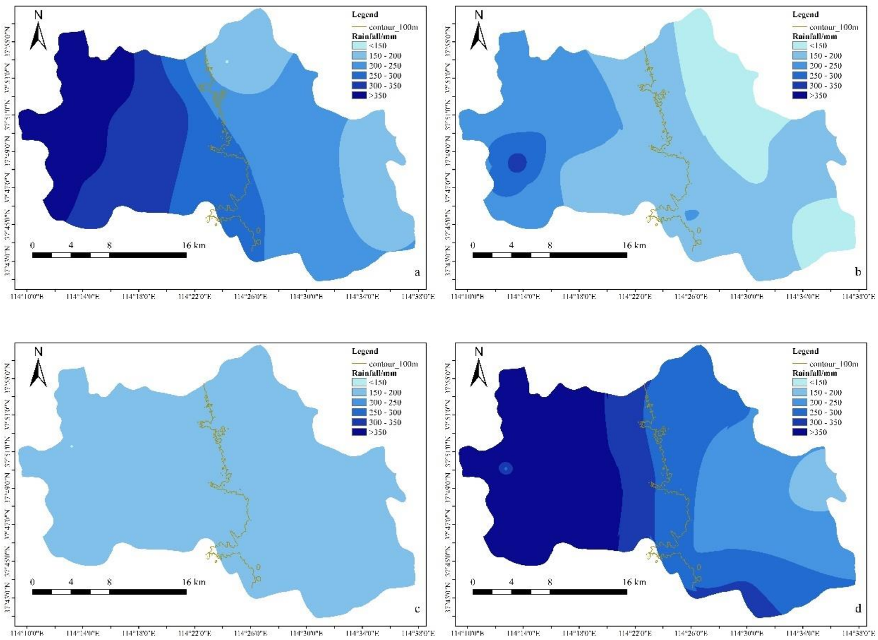

Fig. 4 Spatial distribution of rainfall during (a) July 19 to 24, 2016, (b) July 20 to 25, 2021, (c) October 3 to 10, 2021, and (d) July 29 to August 4, 2023

Further analysis of the relationship between elevation and rainfall at each station for the four rainfall events shows that (Fig. 5) except for this rainfall from October 3 to 10, 2021, there was a significant positive correlation between rainfall and elevation for the remaining three rainfall events.

https://doi.org/10.5194/nhess-2024-8
Preprint. Discussion started: 2 February 2024

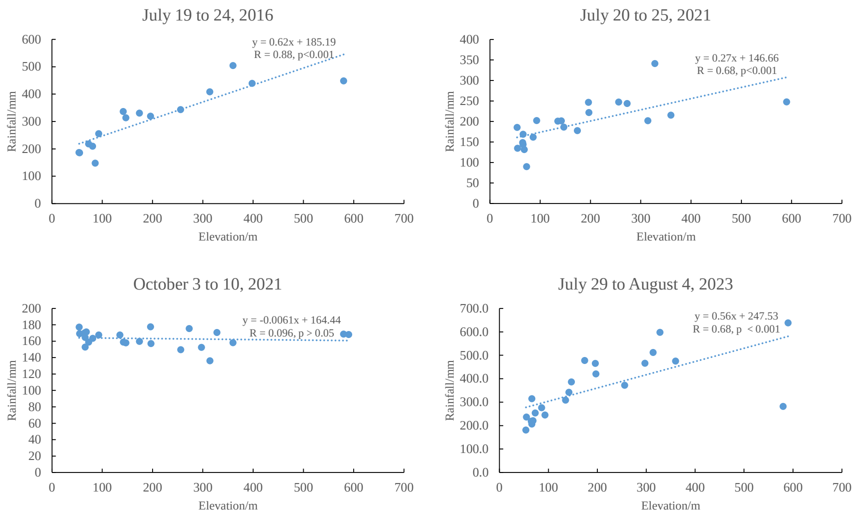

Fig. 5 Correlation analysis between elevation and rainfall during July 19 to 24, 2016, July 20 to 25, 2021, October 3 to 10, 2021, and July 29 to August 4, 2023

Based on the rainfall duration of the four rainfall events, their average rainfall intensities were calculated and converted into 24 h rainfall amounts to show that the spatial variability of rainfall in the Taihang Mountain and the influence of elevation are both smaller when the rainfall during 24 h is lower than 50 mm.

3.3 Surface runoff generating processes

Points plotting the four surface runoff generating processes versus rainfall variations (Fig. 6). For the surface runoff generating process during July 19 to 24, 2016, the rainfall started at 6:00 a.m. on July 19, 2016 and after 12 h of continuous rainfall, by 5:00 p.m. on July 19, 2016 the rainfall accumulated to 100.3 mm, with an intensity of 8.36 mm/h, and began to generate surface runoff, with a flow of 6.44 L/s, and then reached a maximum flow of 185.33 L/s at 1:00 a.m. on July 20, 2016. Followed by 11:00 p.m. on July 20, 2016, the rainfall stopped, at which time the accumulated rainfall

https://doi.org/10.5194/nhess-2024-8
Preprint. Discussion started: 2 February 2024

was 504 mm, lasting 42 h, with an average rainfall intensity of 12.0 mm/h. However, the surface runoff continued to generate, by 1:00 pm on July 24, 2016 the surface runoff ended, lasting 86 h after the rainfall stopped. The surface runoff generating process lasted a total of 117 h, with an average flow of 18.41 L/s, and runoff amounting to 7753 m^3. From 6:00 a.m. on July 19 to 1:00 p.m. on July 24, 2016, the cumulative rainfall was 506.8 mm. The runoff coefficient was 0.58.

For the surface runoff generating process during July 20 to 25, 2021, the rainfall began at 4:00 p.m. on July 20, 2021 and after 32 h of continuous rainfall, by 11:00 p.m. on July 21, the rainfall accumulated to 147.3 mm, and began to generate surface runoff, with a flow of 5.76 L/s, and by 10:00 a.m. on July 22, 2021 the flow reached a maximum value of 8.14 L/s. At the same time, the rainfall stopped and the total rainfall accumulated at this time was 215.4 mm, which lasted for 43 h, with an average rainfall intensity of 5.0 mm/h. While, the surface runoff continued to generate, to 12:00 p.m. on July 25, 2021, the surface runoff ended, lasting 62 h after the rainfall stopped. The surface runoff generating process lasted a total of 73 h, the average flow was 3.07 L/s and runoff amounting to 806 m^3. From 4:00 p.m. on July 20 to 12:00 p.m. on July 25, 2021, the cumulative rainfall was 215.4 mm. The runoff coefficient was 0.14.

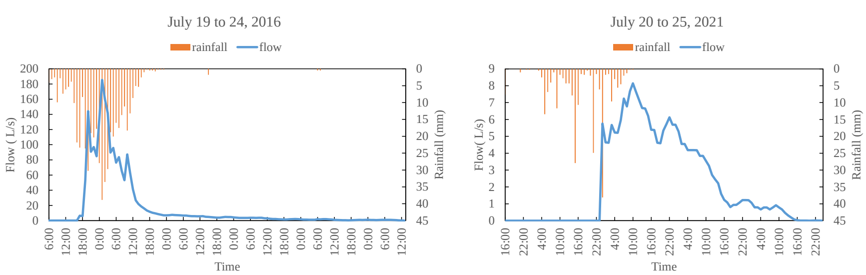

https://doi.org/10.5194/nhess-2024-8
Preprint. Discussion started: 2 February 2024

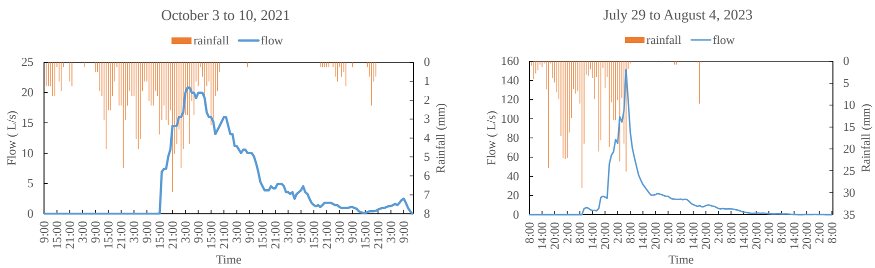

Fig. 6 Surface runoff generating processes during July 19 to 24, 2016, July 20 to 25, 2021, October 3 to 10, 2021, and July 29 to August 4, 2023

For the surface runoff generating process during October 3 to 10, 2021, the rainfall started at 9:00 a.m. on October 3, 2021, and after 55 h of continuous rainfall, by 3:00 p.m. on October 5, 2021 the rainfall accumulated to 85.3 mm, and began to generate runoff with a flow of 0.07 L/s, and then at 4:00 a.m. on October 6, 2021 the flow reached a maximum value of 20.82 L/s, and then by 7:00 p.m. the rainfall stopped, and the total rainfall accumulated at this time was 162.1 mm, which lasted for 83 h, and the average rainfall intensity was 1.95 mm/h, but the runoff continued to generate, and by 3:00 p.m. on October 10, 2021, the flow ended and lasted 90 h after the rainfall stopped. The surface runoff generating process lasted a total of 119 h, the average flow was 6.67 L/s, and runoff amounting to 2859 m^3. From 9:00 a.m. on October 3 to 3:00 p.m. on October 10, 2021, the cumulative rainfall was 173.7 mm. The runoff coefficient was 0.63.

For the surface runoff generating process during July 29 to August 4, 2023, the rainfall started at 8:00 a.m. on July 29, 2023, and after 27 h of continuous rainfall, by 10:00 a.m. on July 30, 2023 the rainfall accumulated to 259.1 mm, and began to produce flow with a flow of 6.20 L/s, and then at 6:00 a.m. on July 31, 2023 the flow reached a maximum of 151.43 L/s, and then by 9:00 a.m., the rainfall stopped, and by this time,

https://doi.org/10.5194/nhess-2024-8
Preprint. Discussion started: 2 February 2024

the cumulative rainfall amounted to 475.3 mm, which lasted for 49 h. The average rainfall intensity was 9.7 mm/h, but the basin continued to produce flow, and by 8:00 a.m. on August 4, 2023, the runoff ended, lasting 96 h after the rainfall stopped. The surface runoff generating process lasted a total of 119 h, with an average flow of 17.14 L/s, and runoff volume of 7342 m^3. From 8:00 a.m. on July 29 to 8:00 a.m. on August 4, 2023, the cumulative rainfall was 487 mm, and the runoff coefficient was 0.57.

3.4 Contributions of precipitation on variation in runoff

We used the surface runoff generating process from July 19 to 24, 2016 as the baseline period (Fig. 7), quantifying the contribution of rainfall to changes in runoff can be obtained based on the double cumulative curve method (Table 2). From Table 2, it can be seen that for the two surface runoff generating processes of October 3 to 10, 2021 and July 29 to August 4, 2023, the contribution of rainfall was more than 100%, and it is inferred that these two surface runoff generating processes were entirely determined by rainfall. In the case of July 20 to 25, 2021, the contribution of rainfall was only 58.17%, while 41.83% of the contribution came from factors other than rainfall. The preliminary inference is the water holding properties of the soil and rock.

https://doi.org/10.5194/nhess-2024-8
Preprint. Discussion started: 2 February 2024

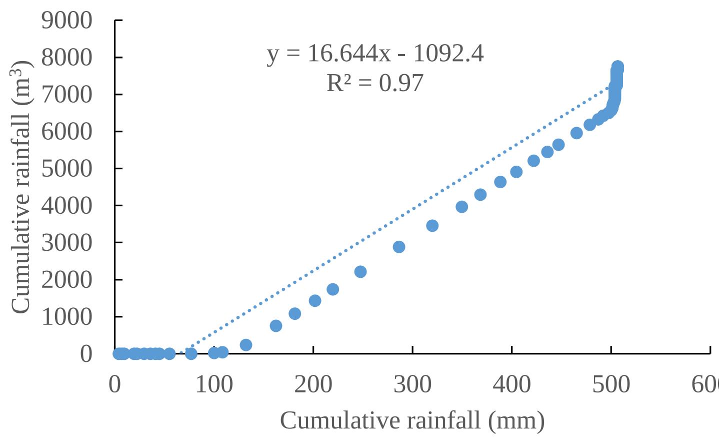

Fig. 7 The double cumulative curve of surface runoff generating process during July 19 to 24, 2016

Table 2 Contribution of rainfall to changes in runoff of four surface runoff generating processes during July 20 to 25, 2021, October 3 to 10, 2021, and July 29 to August 4, 2023

Baseline period	Changing period	$\overline{R_b}$/m^3	$\overline{R_c}$/m^3	T_b/h	T_c/h	$\overline{R_a}$/m^3	ΔP/%
July 19 to 24, 2016		66.27	-	117	-	-	-
	July 20 to 25, 2021	-	11.04	-	73	34.14	58.17
	October 3 to 10, 2021	-	24.03	-	119	15.12	121.09
	July 29 to August 4, 2023	-	61.70	-	119	58.92	160.70

4. Discussion

Based on the analysis of four surface runoff generating processes above, it can be

https://doi.org/10.5194/nhess-2024-8
Preprint. Discussion started: 2 February 2024

seen that in terms of rainfall characteristics, both temporally and spatially, the rainfall characteristics from October 3 to 10, 2021 are completely different from those of the other three surface runoff generating processes. For October 3 to 10, 2021, the average rainfall intensity was 1.46 mm/h. The average rainfall intensity of remaining three surface runoff generating processes were 4.33 mm/h, 2.95 mm/h and 4.09 mm/h, separately. While, it is true that the surface runoff generating process was characterized by July 20 to 25, 2021 as being different from the other three processes. Specifically, for July 20 to 25, 2021, the duration of the surface runoff generating process was only 73 h, and the runoff coefficient was 0.14. For the remaining three periods, the values of duration and the runoff coefficient were both closer, at about 120 h and 0.6 (Table 2). However, the surface runoff generating process during October 3 to 10, 2021 did have the longest time to generate runoff, beginning after the rainfall had lasted 55 h. The reason for these differences is assumed to be related to the infiltration and runoff generation pattern of rainfall.

Runoff generation is the process by which rainfall losses are deducted to form net rainfall. Rainfall losses include vegetative retention, infiltration, infill and evapotranspiration, with infiltration being the most important. Generally speaking, runoff generation is usually generalized into two forms, including (1) runoff resulted from excess rain, which is in the southern humid areas or the northern rainy season, the basin water storage is large, the water table is high, after a rainfall, the basin water storage is easily saturated, which not only generates surface runoff, but also seepage is not all loss, part of which becomes subsurface runoff, so the runoff generation includes

https://doi.org/10.5194/nhess-2024-8
Preprint. Discussion started: 2 February 2024

surface runoff and subsurface runoff; (2) runoff generation under saturated condition, which is in the northern dry areas or the southern rainy season, watershed water storage is less, the groundwater is buried deeper, after a rainfall, the basin water storage is not saturated, the infiltration of all the water is a loss, not the generation of subsurface runoff, only when the intensity of rainfall is greater than the intensity of the infiltration, the rainfall is generated by over-permeation and the surface runoff generates.

Obviously, the four monitored surface runoff processes, the two surface runoff processes in 2016 and 2023 occurred after 12h and 27h of continuous rainfall, respectively, and were typical runoff resulted from excess rain, with the maximum instantaneous flow amounting to 185.33 L/s and 151.43 L/s, respectively, and the average flow amounting to 18.41 L/s and 17.14 L/s, and the duration of the continuous rainfall being 42 h and 49 h, with the average rainfall intensity was 12.0 mm/h and 9.7 mm/h. The rainfall duration was short and the intensity was high, which belonged to the storm runoff. Although the runoff coefficient was about 0.6, this form of runoff did not have any effective supplementation of the soil moisture and subsurface runoff, and did not form effective water resources downstream, which was not very significant for maintaining the local soil water conservation capacity. For semi-arid regions, where rainfall is unevenly distributed over the seasons, more soil water is needed to maintain local and downstream water demand during the non-rainy season.

For the two surface runoff processes in 2021, we inferred that they were both runoff generation under saturated condition. Especially for the surface runoff process from October 3 to 10, 2021, although the runoff generation occurred after 55 h of continuous rainfall, the duration of continuous rainfall was 83 h. The average rainfall intensity was 1.95 mm/h, while the runoff coefficient was 0.63, which is typical runoff generation under saturated condition. This type of runoff generation is generated after the topsoil layer is saturated with soil moisture, and at the same time, a loamy stream is formed inside the topsoil layer to flow in the soil. This explains why, although the rainfall was only 173.7 mm, the runoff generation continued after the rainfall stopped, and the runoff generation duration was comparable to that of the two runoff generation processes in 2016 and 2023 when the rainfall was 506.8 mm and 487 mm. The main reason for this phenomenon is because of the runoff generation in July 2021, the rainfall in this runoff generation process mainly replenishes the soil moisture in the form of infiltration, which is why the rainfall is 215.4 mm, the runoff coefficient is only 0.14, and the average flow rate is 3.07 L/s. From this, we deduce that, for the semi arid areas, the rainfall pattern and the moisture content of the rock and soil are the main factors determining the runoff generation. Under the premise that rainfall conditions can not be changed, for the soil structure characteristics of the soil and rocky mountainous areas, the ability of rock and soil to contain water can be improved by reducing surface runoff, increasing the infiltration capacity of soil moisture, improving soil structure, and increasing the content of soil organic matter, so as to realize the enhancement of water conservation functions in mountainous areas.

The water shortage situation in North China, which is characterized by a significant attenuation of river runoff and an obvious decline in the water table, has been alleviated in the context of the South-to-North Water Diversion, but the

https://doi.org/10.5194/nhess-2024-8
Preprint. Discussion started: 2 February 2024

increasingly serious water ecological problems have not been effectively solved, especially in the mountainous areas of Beijing-Tianjin-Hebei, which are still faced with the dual responsibility of ecological and environmental support zones and the construction of a functional area of water conservation, and have become one of the primary issues to be resolved in the coordinated development of Beijing-Tianjin-Hebei (Wang et al., 2020). How to repair the water ecosystem of the Haihe River Basin and enhance the water-sourcing and nutrient-supporting function of the mountainous areas has become even more important (Xia et al., 2017). The water shortage problem in the North China Plain has now attracted a great deal of attention. China has also initiated a series of water transfer projects, including the South-to-North Water Transfer Project and the Yellow River Diversion and Replenishment of Hebei province (Fig. 8). According to the statistics of the Haihe River Basin Water Resources Bulletin, the proportion of water supplied by inter-basin water transfer projects in the Haihe River Basin's water supply from surface water sources is about 50%. The ratio of external water transfers to total water supply increases from 17.6% in 2016 to 30.2% in 2021 (Haihe Water Resources Commission, 2022).

However, for the North China Plain, the lack of water can be transferred. The disasters caused by the unpredictable rainstorm weather, like torrential floods, flash floods and geologic disasters and urban waterlogging, etc., are immeasurable. Taking July 19, 2016 as an example, this rainstorm weather led to 142 counties in Hebei Province were affected by the disaster, the affected population was 7.433 million, the number of deaths was 36, and the missing population was 77, the rainstorm process

https://doi.org/10.5194/nhess-2024-8
Preprint. Discussion started: 2 February 2024

also led to a large number of house collapses, and the direct economy due to the disaster was as high as 8.973 billion RMB yuan, which led to the affected area of crops was as high as 604.1 khm^2 , and the area of crops that had gone out of harvest was 18.1 khm^2 (Zhu et al., 2019).

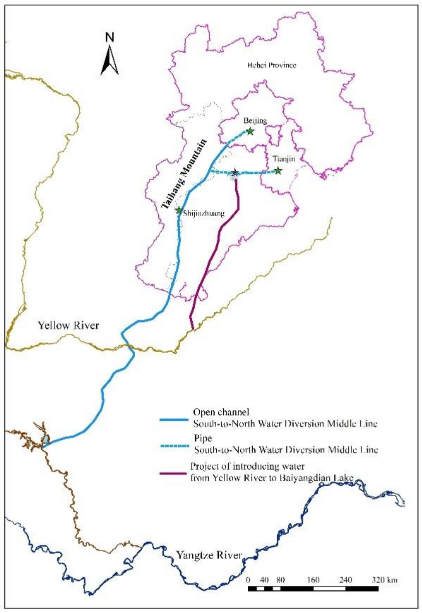

Fig. 8 Schematic diagram of different water transfer projects in the North China Plain

The community of life in the mountains, waters, forests, fields, lakes and seas, which profoundly reveals the fundamentals of the life process of man and nature, is an organic whole of energy flow, material circulation and information transmission among different natural ecosystems, and is also a life organism that is closely dependent on mankind, rich in biodiversity and with a larger regional scale. Integral protection, systematic restoration and comprehensive management should be carried out. On the basis of the existing Yellow River water as the water source in the Beijing-Tianjin-Hebei region, the water line in the Yangtze River and the east line of the Yangtze River

https://doi.org/10.5194/nhess-2024-8
Preprint. Discussion started: 2 February 2024

are fully utilized as the external inputs to the Beijing-Tianjin-Hebei region, so as to alleviate the pressure on the regional water supply, and to provide a basic guarantee for the safety of drinking water. At the same time, the water production performance, water containment performance, water resources utilization rate and water purification capacity within the basin will be enhanced from four aspects: water production, water containment, water conservation and water purification. Through the synergistic effect of external and internal, the goal of sustainable drinking water health is achieved. Eventually, a water ecological corridor will be constructed to control groundwater overexploitation and appropriately restore groundwater, safeguard ecological base flow, and form a "mountains, water, forests, fields, lakes, and seas" water ecological pattern (Cao et al., 2019).

Changes in rainfall patterns directly lead to changes in runoff generation of small mountain watersheds. When extreme rainfall events occur, only by preventing is unable to ensure the ecological security of the downstream plains and water security, but also need to be managed from the source, people should pay attention to further clarification of the intrinsic mechanisms of hydrological processes in mountainous areas and the importance of the factors that influence them as a whole, including the surface runoff generation process, the soil and rock infiltration process and the subsurface runoff generation process, and so on. From the perspective of the Earth's critical zone, a comprehensive approach should be taken into consideration, in order to give full play to the important ecological function of the mountainous areas of the water and soil conservation and maintenance of the water source.

https://doi.org/10.5194/nhess-2024-8
Preprint. Discussion started: 2 February 2024

5. Conclusions

In this study, the surface runoff generation processes differed among the different heavy rainfall events in the Taihang Mountain. Frequency of extreme weather years is dominant from 2014 to 2023. The heavy rainfall shows obvious spatial distribution, the rainfall dividing line of rainfall greater than 200 mm basically coincides with the 100 m contour line. The spatial variability of rainfall in the Taihang Mountain and the influence of elevation are both smaller when the rainfall during 24 h is lower than 50 mm.

The two surface runoff processes in 2016 and 2023 were typical runoff resulted from excess rain, which belonged to the storm runoff. The two surface runoff processes in 2021 were runoff generation under saturated condition. For runoff generation under saturated condition, the contribution of rainfall was only 58.17%. While when the runoff coefficient was greater than 0.5, the surface runoff generating processes were entirely determined by rainfall. For semi-arid regions, where rainfall is unevenly distributed over the seasons, more soil water is needed to maintain local and downstream water demand during the non-rainy season. For the soil structure characteristics of the soil and rocky mountainous areas, the ability of rock and soil to contain water can be improved by reducing surface runoff, increasing the infiltration capacity of soil moisture, improving soil structure, and increasing the content of soil organic matter. The result of this study is so of great significance for realizing the enhancement of water conservation functions in mountainous areas of north China.

Acknowledgements

This work was supported by the Science &Technology Fundamental Resources Investigation Program (2022FY100104), the Natural Science Foundation of Hebei Province (D2021503001), the National Natural Science Foundation of China (42371048), and the Key Research and Development Plan Project of Hebei Province (22324202D).

Author contribution

Writing—original draft, Hui Yang; Writing—review and editing, Jiansheng Cao and Xianglong Hou. All authors have read and agreed to the published version of the manuscript.

Competing Interest

The authors declare that they have no known competing financial interests or personal relationships that could have appeared to influence the work reported in this paper.

Data availability

Data is contained within the paper.

References

[1] Cao, J.S., Yang, H., Zhao, Y., 2021. Experimental analysis of infiltration process and hydraulic properties in soil and rock profile in the Taihang Mountains, North China. Water Supply, 22(2), 1691.

[2] Cao, J.S., Liu, C.M., Zhang, W.J., Han, S.M., 2013. Using temperature effect on seepage variations as proxy for phenological processes of basin-scale vegetation communities. Hydrological Processes, 27, 360-366.

[3] Cao, X.F., Hu, C.Z., Qi, W.X., Zheng, H., Shan, B.Q., Zhao, Y., Qu, J.H., 2019. Strategies for Water Resources Regulation and Water Environment Protection in Beijing–Tianjin–Hebei Region. Strategic Study of CAE, 21(5), 130-136. (in Chinese with English abstract)

[4] Chen, H., Zhang, X., Abla, M., Lü, D., Yan, R., Ren, Q., Ren, Z., Yang, Y., Zhao, W., Lin, P., Liu, B., Yang, X., 2018. Effects of vegetation and rainfall types on surface runoff and soil erosion on steep slopes on the Loess Plateau, China. Catena, 170, 141-149.

[5] Chen, J.X., Zou, G.R., Yin, W.S., Zheng, H.R., 1984. Irrigation District Water Measurement Workbook. Water Resources and Hydropower Press, Beijing, in Chinese.

[6] Cheng, S., Yu, X.X., Li, Z.W., Xu, X.L., Ding, M.M., 2022. Using four approaches to separate the effects of climate change and human activities on sediment discharge in karst watersheds. Catena, 212, 106118.

[7] Conrad, V., Pollak, C., 1950. Methods in Climatology. Harvard University Press, Cambridge.

[8] Du, J.K., Jia, Y.W., Hao, C.P., Li, X.X., Qiu, Y.Q., Niu, C.W., 2018. Evolution law and attribution analysis of vertical distribution of blue water and green water in Taihang Mountain region. South-to-North Water Transfer and Water Science and Technology, 16(2), 64-73. (in Chinese with English abstract)

[9] Fei, K., Deng, L., Zhang, L., Sun, T.Y., Wu, Y.H., Fan, X.J., Dong, Y.Y., 2019. Lateral transport of soil total carbon with slope runoff and interflow: effects of rainstorm characteristics under simulated rainfall. Catena, 179, 39-48.

[10] Fu, T.G., Liu, J.T., Gao, H., Qi, F., Wang, F., Zhang, M., 2023. Surface and subsurface runoff generation processes and their influencing factors on a hillslope in northern China. Science of the Total Environment, 906, 167372.

[11] Gao, P., Li, P.F., Zhao, B.L., Xu, R.R., Zhao, G.J., Sun, W.Y., Mu, X.M., 2017. Use of double mass curves in hydrologic benefit evaluations. Hydrological Processes, 31, 4639-4646.

[12] Geng, S.B., Shi, P.L., Zong, N., Zhu, W.R., 2018. Using soil survey database to assess soil quality in the heterogeneous Taihang mountains, North China. Sustainability, 10 (10), 3443.

[13] Geng, S.B., Shi, P. L., Song, M.H., Zong, N., Zu, J.X., Zhu, W.R., 2019. Diversity of vegetation composition enhances ecosystem stability along elevational gradients in the Taihang Mountains, China. Ecological Indicators, 104, 594-603.

[14] Gocic, Trajkovic, 2013. Analysis of changes in meteorological variables using Mann-Kendall and Sen's slope estimator statistical tests in Serbia. Global and Planetary Change, 100, 172-182.

[15] Haihe river water resources bulletin 2021, 2022. Haihe River Water Conservancy Commission, MWR, Beijing. (In Chinese)

[16] Hirabayashi, Y., Mahendran, R., Koirala, S., Konoshima, L., Yamazaki, D., Watanabe, S., Kanae, S., 2013. Global flood risk under climate change. Nature Climate Change, 3(9), 816-821.

[17] Huntington, T. G., 2006. Evidence for intensification of the global water cycle: Review and synthesis. Journal of Hydrology, 319(1-4), 83-95.

[18] Jing, X., Li, L., Chen, S., Shi, Y.L., Xu, M.X., Zhang, Q.W., 2022. Straw returning on sloping farmland reduces the soil and water loss via surface flow but increases the nitrogen loss via interflow. Agriculture, Ecosystems & Environment, 339, 108154.

[19] Jia, Y.W., Hao, C.P., Niu, C.W., Qiu, Y.Q., Du, J.K., Xu, F., Liu, H., 2019. Spatial-temporal variations of precipitation and runoff and analyses of water-heat-human-land matching

characteristics in a typical mountainous area of China. Acta Geographica Sinica, 74(11), 2288-2302 (in Chinese with English abstract).

[20] Ju, X.H., Li, W.F., Li, J.R., He, L., Mao, J.Q., Han, L.J., 2023. Future climate change and urban growth together affect surface runoff in a large-scale urban agglomeration. Sustainable Cities and Society, 99, 104970.

[21] Kendall, M.G., 1975. Rank Correlation Methods. Charles Griffin, London.

[22] Li, L., Song, X., Xia, L., Fu, N., Feng, D., Li, H., Li, Y., 2020. Modelling the effects of climate change on transpiration and evaporation in natural and constructed grasslands in the semi-arid Loess Plateau, China. Agriculture, Ecosystems & Environment, 302, 107077.

[23] Liu, G., Wang, G., 2012. Insight into runoff decline due to climate change in China's Water Tower. Water Science and Technology: Water Supply, 12(3), 352-361.

[24] Maier, F., van Meerveld, I., Weiler, M., 2021. Long-term changes in runoff generation mechanisms for two proglacial areas in the Swiss Alps II: subsurface flow. Water Resources Research, 57 (12), e2021WR030223.

[25] Mann, H.B., 1945. Nonparametric tests against trend. Econometrica 13(3), 245.

[26] Martínez-Mena, M., Carrillo-Lopez, ´ E., Boix-Fayos, C., Almagro, M., García Franco, N., Díaz-Pereira, E., Montoya, I., de Vente, J., 2020. Long-term effectiveness of sustainable land management practices to control runoff, soil erosion, and nutrient loss and the role of rainfall intensity in Mediterranean rainfed agroecosystems. Catena, 187, 104352.

[27] Mohamadi, M.A., Kavian, A., 2015. Effects of rainfall patterns on runoff and soil erosion in field plots. International Soil and Water Conservation Research, 3, 273-281.

[28] Najafi, M., Zhang, Y., Martyn, N., 2021. A flood risk assessment framework for interdependent

infrastructure systems in coastal environments. Sustainable Cities and Society, 64, 102516.

[29] Pour, S.H., Abd Wahab, A.K., Shahid, S., Asaduzzaman, M., Dewan, A., 2020. Low impact development techniques to mitigate the impacts of climate-change-induced urban floods: Current trends, issues and challenges. Sustainable Cities and Society, 62, 102373.

[30] Qi, F., Liu, J., Gao, H., et al., 2023. Characteristics and spatial–temporal patterns of supply and demand of ecosystem services in the Taihang Mountains. Ecological Indicators, 147, 109932.

[31] Ran, Q., Su, D., Li, P., He, Z., 2012. Experimental study of the impact of rainfall characteristics on runoff generation and soil erosion. Journal of Hydrology, 424–425, 99-111.

[32] Sakakibara, K., Tsujimura, M., Song, X. F., Zhang, J., 2017. Spatiotemporal variation of the surface water effect on the groundwater recharge in a low-precipitation region: application of the multi-tracer approach to the Taihang Mountains, North China. Journal of Hydrology, 545, 132-144.

[33] Silva, R.M., Santos, C.A.G., Moreira, M., Corte-Real, J., Silva, V.C.L., Medeiros, I.C., 2015. Rainfall and river flow trends using Mann-Kendall and Sen's slope estimator statistical trends in the Cobres River basin. Nature Hazards, 77, 1205-1221.

[34] Singh, V.P., 1998. Log-Pearson Type III Distribution BT - Entropy-based Parameter Estimation in Hydrology. Springer, Netherlands.

[35] Swed, F.S., Eisenhart, C., 1943. Tables for testing randomness of grouping in a sequence of alternatives. Annals of the Institute of Statistical Mathematics, 14(1), 66-87.

[36] Wang, J., Chen, W.W., Qi, S.L., Zhou, C.H., Zhang, W.J., 2014. Spatial analysis of soil and water loss sensitivity based on USLE and GIS – a case study of Taihang Mountain area in Hebei Province. Geographical Research, 614-624. (in Chinese with English abstract)

https://doi.org/10.5194/nhess-2024-8
Preprint. Discussion started: 2 February 2024

[37] Wei, W., Jia, F., Yang, L., Chen, L., Zhang, H., Yu, Y., 2014. Effects of surficial condition and rainfall intensity on runoff in a loess hilly area, China. Journal of Hydrology, 513, 115-126.

[38] Xia, J., Zhang, Y.Y., 2017. Water resource and pollution safeguard for Xiongan New Area construction and its sustainable development. Bulletin of Chinese Academy of Sciences, 32(11), 1199-1205. (in Chinese with English abstract)

[39] Yang, H., Hou, X.L., Cao, J.S., 2023. Identifying the driving impact factors on water yield service in mountainous areas of the Beijing-Tianjin-Hebei Region in China. Remote Sensing, 15, 727.

[40] Yang, Y.Y., 2021. Evolution of habitat quality and association with land-use changes in mountainous areas: A case study of the Taihang Mountains in Hebei Province, China. Ecological Indicators, 129, 107967.

[41] Yavuz Selim Gülü, 2020. Improved visualization for trend analysis by comparing with classical Mann-Kendall test and ITA. Journal of Hydrology, 584, 124674.

[42] Yoon, J., Wang, S., Gillies, R. R., Kravitz, B., Hipps, L., Rasch, P., 2015. Increasing water cycle extremes in California and in relation to ENSO cycle under global warming. Nature Communications, 6, 8657.

[43] Zhao, J.C., Zhang, J.J., Hu, Y.W., Li, Y., Tang, P., Gusarov, A.V., Yu, Y., 2022. Effects of land uses and rainfall regimes on surface runoff and sediment yield in a nested watershed of the Loess Plateau, China. Journal of Hydrology: Regional Studies, 22, 404277.

[44] Zhang, N., Ge, Y.W., Li, Y.C., Li, B., Zhang, R.C., Zhang, Z., Fan, B.S., Zhang, W.S., Ding, G.Q., 2021. Modern pollen-vegetation relationships in the Taihang Mountains: towards the quantitative reconstruction of land-cover changes in the North China Plain. Ecological

https://doi.org/10.5194/nhess-2024-8
Preprint. Discussion started: 2 February 2024

Natural Hazards and Earth System Sciences Discussions

Indicators, 129, 107928.

[45] Zheng, H., Chiew, F. H. S., Charles, S., Podger, G., 2018. Future climate and runoff projections across South Asia from CMIP5 global climate models and hydrological modelling. Journal of Hydrology: Regional Studies, 18, 92-109.

[46] Zheng, H., Miao, C., Zhang, G., Li, X., Wang, S., Wu, J., Gou, J., 2021. Is the runoff coefficient increasing or decreasing after ecological restoration on China's Loess Plateau? International Soil and Water Conservation Research, 9, 333-343.

[47] Zhu, Z.W., 2019. Analysis of the July 18-19, 2016 heavy rain process in Hebei Province. Practical rural technology, 3,17. (In Chinese)